Performance of Glare panels subjected to intense pressure pulse loading

C. Soutis
c.soutis@sheffield.ac.uk
G. Mohamed
g.mohamed@sheffield.ac.uk
A. Hodzic
a.hodzic@sheffield.ac.uk
The University of Sheffield
Sheffield, UK

ABSTRACT

A robust and efficient computational model has been developed which is capable of modelling the dynamic non-linear behaviour of Glare panels subjected to blast loadings. High strain rate material characterisation and modelling of interfacial debonding between adjacent sublaminates have been taken into consideration. Numerical model validation have been performed considering case studies of Glare panels subjected to a blast-type pressure pulse for which experimental data on the back face- displacement and post-damage observations were available. Excellent agreement of mid-point deflections and evidence of severe yield line deformation were shown and discussed against the performed blast tests. A further parametric study identified Glare as a potential blast attenuating structure, exhibiting superior blast potential against monolithic aluminium plates. The results were normalised and showed that for a given impulse, Glare exhibited a smaller normalised displacement, outperforming monolithic Aluminium 2024-T3 plates. It was concluded that further work needed to be carried out to take into account the influence of geometry (cylindrical structures), pre-pressurisation effects and boundary conditions

Paper No. 3715. Manuscript received 5 May 2011, revised version received 12 July 2011, accepted 11 November 2011.

https://doi.org/10.1017/S0001924000007120 Published online by Cambridge University Press

NOMENCLATURE

A	strain hardening constant
B	strain hardening coefficient
C	strain rate coefficient
C_p	specific heat capacity
E	Young's modulus
E_{ij}	laminate stiffness in ij direction
G_{ij}	laminate shear stiffness
I	impulse
L	plate length
n	strain hardening exponent
m	thermal softening exponent
P	pressure
P_0	peak pressure
R_0	explosive charge radius
S	stand-off distance
$S_{LT,TT}$	in-plane shear failure stress
t_0	exponential time decay constant
T	temperature
T_{melt}	melting temperature
T_{room}	room temperature
W	plate width
X_c	longitudinal compressive strength in fibre x-direction
X_t	longitudinal tensile strength in fibre x-direction
Y_c	transverse compressive strength in y-direction
Y_t	transverse tensile strength in y-direction
ρ	mass density
σ	characteristic material stress
$\bar{\sigma}$	effective stress
$\bar{\varepsilon}^p$	effective plastic strain,
$\dot{\varepsilon}$	total strain rate
ε_0	reference plastic strain rate
α_q	non-dimensional impulse
υ	Poisson's ratio

1.0 INTRODUCTION

Composite materials have gained popularity in high performance products that need to be lightweight, yet strong enough to take high loads such as aerospace structures (tails, wings and fuselages)[1]. Glare (GLAss fibre REinforced laminate) is a class of fibre-metal laminates (FMLs) for advanced aerospace structural applications. It consists of thin aluminium 2024-T3 sheets bonded together with unidirectional or biaxially reinforced adhesive pre-preg of high strength glass fibres (S2-glass/FM94). Developed as a lightweight alternative to structural metals, Glare offers a unique combination of, amongst many others; outstanding fatigue resistance, ease of manufacture and repair[2]. As a result, Glare is an attractive hybrid system for lightweight, fatigue critical structural applications, currently used in the manufacture of the upper fuselage skin structure of the Airbus A380[2].

https://doi.org/10.1017/S0001924000007120 Published online by Cambridge University Press

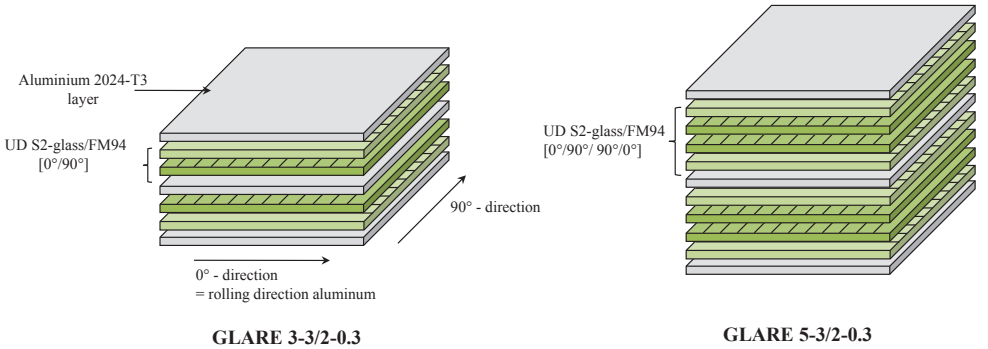


Figure 1. Configuration of Glare laminates: (left) 3-2/1 and (right) 5-3/2.

However, Glare also exhibits excellent impact properties and enhance energy absorption, relative to monolithic aluminium of the same areal density[3,4], suitable for structural components susceptible to damage from foreign object projectiles (i.e. runaway debris/bird-strike/sabotage). Although various Glare configurations exists, depending on the structural requirements, it is the cross-plied Glare 3 and Glare 5 with bi-directional reinforcement which has been identified as possessing the best impact characteristics, see Table 1 and Fig. 1 for details[2]. Hoo Fatt *et al*[4] developed analytical solutions to predict the ballistic limit and energy absorption of fully clamped Glare 5 panels. The analytical model estimated the amount of energy absorbed by the different failure and damage mechanisms in the panels. The energy partition reported for 'thin' and 'thick' panels attributed only 2-9% of the total energy to delamination effects. The most significant proportion of the energy (92-84%) was attributed to bending and membrane energy. The epoxy-based composite used in GALRE 5 resulted in a 15% increase in the ballistic limit compared to plain 2024-T3 aluminium alloy. Vlot *et al*[3] attributed the increase in energy absorption of Glare to the high strain rate phenomenon that occurs in glass fibres combined with their relatively high failure strain, since such an increase would not be as significant in bare aluminium. This complex strain rate dependent behaviour was further investigated by work presented by McCarthy *et al*[5], which developed a strain rate dependent continuum damage mechanics model to simulate a bird strike on a Glare 3 aircraft wing leading edge.

Table 1
Commercially available fibre-metal laminates for fatigue and impact applications[2]

	Grade	Metal type	Metal thickness (mm)	Fibre layer (mm)	Fibre direction (°)	Characteristics
Glare	3	2024-T3	0·2 – 0·5	0·266	0º/90°	Fatigue, impact
	5	2024-T3	0·2 – 0·5	0·5	0º/90°/90º/0°	Impact

The structural response of Glare to blast type loading has also received some attention in recent years, in response to the growing threat of sabotage to primary aerospace structures. In response to the Pan Am Flight 103 Lockerbie air-disaster, a series of hardened luggage containers made from a variety of materials, including reinforced aluminium, fibre glass and polymers were tested to meet Federal Aviation Administration (FAA) standards[6,7]. Glare was the only material to pass certification with no reported breaching of the container. The Glare structure was able to

https://doi.org/10.1017/S0001924000007120 Published online by Cambridge University Press

withstand and absorb the explosive energy, greater than that in the Lockerbie air disaster, and redistribute the impact load to the adjacent surface area rather than to one specific weak spot[7]. Although significant deformation was present, the overall container remained intact. Within the EU-funded VULCAN programme (AST5-CT-2006-031011), three aerospace structural materials were selected for blast assessment using small-scale blast trials[8]. The relative performance of the candidate materials was assessed in terms of the threshold charge weight for a fixed stand-off distance, defined as the charge weight of explosive required to cause maximum damage without through-thickness rupture. Small-scale testing was undertaken using 800mm × 800mm targets. In order to replicate the highly focussed loading associated with an aircraft on-board explosion event and minimise the influence of boundary effects, a standoff distance of 200mm was employed. The level of blast loading (in terms of peak overpressure and impulse) was controlled by varying the mass of the spherical charge. The results of the small-scale blast tests reveal that for a given explosive charge, Glare 3 panels outperformed Aluminium 2024-T3 and CFRP panels. The Aluminium plates indicated a failure limit between 80g and 85g. For Glare, the authors claim a failure limit greater than 150g C-4, although no rupture was reported other than pulling-in of the panel edges proceeded by significant tearing of the bolt holes. This feature was also observed by similar tests performed by Langdon *et al*[9] on fully clamped Glare 3 subjected to PE4 plastic explosives. This raises doubts about the load charge required to produce tearing as these features may have delayed the onset of tearing at the clamped boundary conditions. The influence of boundary conditions is extremely important and has implications for model representation in numerical simulations and analytical modelling. Results presented by Langdon *et al*[9] indicate that the Glare 3 panels behave similarly to monolithic metal plates, exhibiting large plastic deformation and yield line formation. The tests showed a trend of increasing normalised displacement with increasing non-dimensional impulse. The panels appeared to offer potential blast resistance when compared to monolithic mild steel plates. At a stand-off distance (SOD) of 200mm, no significant through-thickness rupture or petalling was observed for the maximum PE4 plastic explosive charge of 31·9g. To the author's knowledge no numerical studies have been performed to validate this study.

Small-scale experimental trials are important in establishing benchmark behaviour of structural materials to blast-type loading. However, such experiments are expensive and time-consuming and are not amenable to cover different lay-up configurations, loading regimes and boundary conditions. Modelling the behaviour of these structural materials, using commercial finite element software, would be of great assistance as only a small number of experimental tests would need to be performed for model verification and validation. This requires developing efficient and reliable predictive techniques which takes into account accurate material characterisation, appropriate failure criteria and description of the blast loads. This would enable the response of larger components (e.g. fuselage or aircraft luggage containers) to be modelled without the need to undertake a large number of experimental tests. Numerical work performed by Karagiozova *et al*[10] on polypropylene based FMLs[11], has shown that it is possible to simulate and capture the response and failure mechanisms to localised blast loading using commercial finite element software.

The objective of this paper is to present a robust and computationally efficient predictive model which can capture the dynamic non-linear behaviour of FMLs using the explicit finite element code LS-DYNA[12], based on the aforementioned tests of Langdon *et al*[9], for which experimental data on the back face-displacement and post-damage information is available for model validation.

The structure of the paper is as follows: Section 2 provides a brief description of the experi-

https://doi.org/10.1017/S0001924000007120 Published online by Cambridge University Press

mental blast tests; Section 3 outlines the numerical methodology with reference to choice of numerical algorithms, derivation of appropriate high strain-rate material properties and predicting the spatial and time response of the blast explosive. The developed predictive model is validated against experimental data and compared against other Glare variants and equivalent monolithic metallic panels, described in Section 4.

2.0 BLAST TEST DESCRIPTION

The Glare 3 panels investigated by Langdon *et al*[9] are 1·42mm thick and comprise of three 0·3mm thick aluminium 2024-T3 alloy sheets, with two cross-plied (0°/90°) unidirectional S2-glass/FM94 between each pair of aluminium sheets. The square panels of dimensions 300mm × 300mm were clamped between two steel frames and mounted onto a ballistic pendulum during blast testing, leaving an area exposed of 200mm by 200mm. The mass of the disc-shape PE4 plastic explosive was varied between 4g to 14g to change the impulse applied to the panels. Due to the low thickness of the Glare 3 panel, severe damage and petalling was observed for low impulses due to the localised nature of the blast load. To increase the spatial uniformity and decrease the intensity of the blast wave, a square tube, shown in Fig. 2, was employed to site the explosive 200mm away from the panel. The explosive was detonated at the open end of the tube and the blast wave was directed down the tube towards the specimen. Two charge diameters (20mm, 40mm) were used, both of which resulted in uniform type response of the Glare 3 panels. The results of the experiment are shown in Table 2.

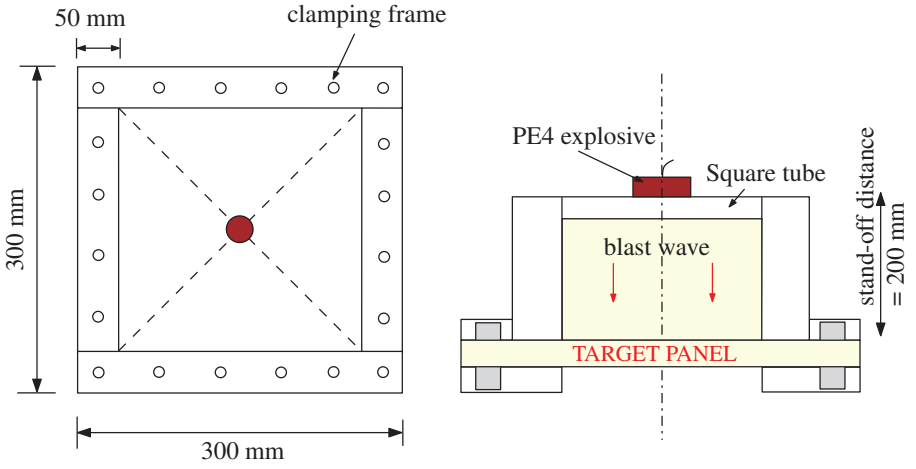


Figure 2. Schematic of experimental small-scale blast trials performed by in Langdon *et al*[9].

https://doi.org/10.1017/S0001924000007120 Published online by Cambridge University Press

Table 2
Schematic of blast square tube blast set-up used in Langdon and co-workers experiment[9]

Panel	Stand-off distance (mm)	Explosive charge diameter (mm)	Charge mass (g)	Impulse (Ns)	Back-face displacement (mm)	*d/t* (–)
1	200	40	14	31·9	31·2	21·97
2	200	40	11	28	26·7	18·8
3	200	40	9	25·5	24·1	16·97
4	200	40	7	21·3	21·3	15
5	200	40	5	17·3	17	11·97
6	200	20	5	13·1	10·9	7·68
7	200	20	3	11	9·4	6·62

3.0 NUMERICAL MODELLING

3.1 2D modelling rationale

FMLs are expected to fail under a multitude of failure mechanisms which are akin to those found in both metallic and composite structures. Such failure may involve severe plastic deformation, interlaminar debonding, and intralaminar damage such as fibre breakage and matrix cracking, all of which should be captured by the proposed computational model. The manifestation of these failure mechanisms will depend, amongst many others, on the nature of the dynamic loading (spatial intensity of the blast wave) and the applied edge boundary conditions which are imposed on the test panels as a result of clamping. The latter may prevent vibratory interference with the blast shock waves, resulting in more pronounced through-thickness perforation and shear damage. These factors will indeed influence and preclude the use of certain element formulations and constitutive models and require a different finite element modelling rationale.

The tested Glare panels from both experimental studies had a nominal thickness on the order of a few millimeters, whereas the panels had a quadrangular geometry of the order of a few hundred millimetres ($t/L \approx 0{\cdot}004$). Additionally, the blast load duration of the pressure-pulse loading is much higher than the transition time for through-thickness shock waves; hence the response of the panel is dominated by two-dimensional, transverse shear waves. The uniaxial strain wave speed in a cross-plied 0º/90° orthotropic and homogeneous metallic plates was evaluated to be approximately $C_{comp} \approx 3{,}700\text{ms}^{-1}$ and $C_{al} \approx 3{,}130\text{ms}^{-1}$. As the wave transit time through each layer can be defined as $t = h/C_{comp}$, and since all of the damaged Glare panels from the experiments underwent extensive panel deformation before tensile tearing, it is therefore reasonable to assume that the through-thickness stress-waves can be considered negligible in thin FML panels. Due to this large aspect ratio with respect to the laminate thickness and two-dimensional transverse shear wave assumption, each layer can be assumed to be in state of plane stress, with all through-thickness normal and shear components of the stress tensor (σ_{13}, σ_{23}, σ_{33}) are assumed to be negligible in comparison with their in-plane counterparts (σ_{11}, σ_{22}, σ_{12}). As the mechanical properties of this hybrid system vary between each subsequent laminate, each layer can be represented by a unique set of integration

https://doi.org/10.1017/S0001924000007120 Published online by Cambridge University Press

points, as in the case of shell elements. Although this approach neglects interfacial debonding between adjacent layers, this assumption is acceptable if no considerable debonding is observed from post-damaged cross-section samples[9]. In LS-DYNA there are several options for modelling layered composites with shell elements. For this study the *PART_COMPOSITE card was chosen to model the hybrid layers of Glare 3 with fully integrated shell elements (Type 16). This card allows the user to assign materials ID's, material orientation and thickness to a unique integration point. The total thickness of the composite shell is the sum of the integration point thickness.

This planar assumption is valid for most thin-walled composite structures, but breaks down in several specific instances, such as thick composite systems where the laminate thickness is no longer negligible in comparison with the other dimensions, and interlaminar through-thickness stress tensor components must be considered.

Numerical geometry in numerical simulation is the same as those in the experimental set-up. Due to symmetry conditions and reduced computational constraints, only 1/4 of the plate is modelled. It is assumed that the panel is perfectly clamped along the outer boundary edges, neglecting any interaction between the FML panel and steel clamp plates.

3.2 High strain rate material properties

Typical quasi-static stress strain curves from static tensile tests for Glare 3 and its constituents are shown in Fig. 3. While quasi-static material data is widely available in the open literature, accurate high strain rate material characterisation for Glare 3 is scarce which poses challenges to the numerical analyst when defining input parameters for damage constitutive models.

3.2.1 S2-glass/FM94

In the open literature, high strain rate tensile tests on FML specimens (Glare 3-3/2-0·4) showed very little evidence for rate dependency (up to 3,300s^{-1}) for any of the in-plane elastic

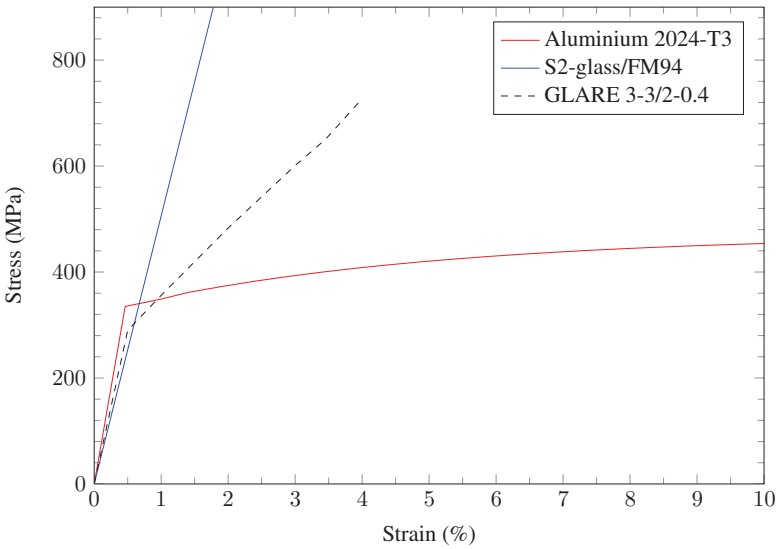


Figure 3. Typical tensile stress-strain curves of Glare and its constituents – Aluminium 2024-T3 and S2-glass/FM9.

https://doi.org/10.1017/S0001924000007120 Published online by Cambridge University Press

properties[5]. However tensile strength tests on 0° FML waisted specimens have shown an increase in ultimate load capacity (tensile strength) of 19% for quasi-static to to 3,300s^{-1} rates. To account for the strain rate effects observed in the experiments, McCarthy *et al*[5] assigned a Dynamic Increase Factor (DIF) to the numerical strain rate model assuming that the transverse modulus, shear modulus and longitudinal fibre rupture strains were rate dependent and the longitudinal Young's modulus of the glass composite layers were not. Similarly, Hoo Fatt *et al*[4] assumed that the in-plane elastic properties were 1·5 times that of the static values, although the Poisson's ratios remained equal to the static equivalent.

Considering the incomplete data available for the individual constituents of the Glare (particularly the glass layers), and strain rate independent failure criteria available in LS-DYNA, quasi-static in-plane elastic and strength properties were assumed, taken from Refs 13 and 14, respectively. However, the maximum fibre rupture strain in tension was increased by a factor of 2·02 (as chosen by McCarthy *et al*[5]), to match the failure strain of Glare 3 at the maximum strain rate of 3,300s^{-1}.

The composite material behaviour was modelled with *MAT_54 (ENHANCED_COMPOSITE_DAMAGE with optional failure criteria of Chang and Chang[15] or Tsai and Wu[16]. In this study, the Chang and Chang failure criterion was applied and laminated shell theory was activated to properly model the transverse shear deformation. The material properties used for *MAT_54 are shown in Table 3.

Table 3
Material property data used to represent S2-glass/FM94 laminates[13,14]

*MAT_ENHANCED_COMPOSITE_DAMAGE
MAT_054

Property	Units	Value	Strength	Units	Value
ρ	kg/m^3	1,980	S_{LT}	MPa	75
E_{11}	GPa	50·6	S_{TT}	MPa	50
E_{22}	GPa	9·9	X_C	MPa	2,000
E_{33}	GPa	9·9	Y_C	MPa	150
υ_{12}	–	0·32	X_T	MPa	2,500
υ_{12}	–	0·32	Y_T	MPa	50
υ_{12}	–	0·063			
G_{12}	GPa	3·7			
G_{13}	GPa	3·7			
G_{23}	GPa	1·65			

3.2.2 Aluminium 2024-T3

To describe the elastic-plastic response of the Aluminium 2024-T3 layers, an isotropic constitutive model based on the Johnson-Cook material model[17] was implemented, as shown in Equation (1).

$$\sigma_y = \left(A + B\bar{\varepsilon}^p\right)^n \left[1 + C\ln\left(\frac{\dot{\varepsilon}}{\dot{\varepsilon}_0}\right)\right]\left[1 - \left(\frac{T - T_{room}}{T_{melt} - T_{room}}\right)^m\right] \quad \ldots (1)$$

https://doi.org/10.1017/S0001924000007120 Published online by Cambridge University Press

Normally for high rate deformation problems, it is assumed that 90-100% of the plastic work is dissipated as heat in the material[18]. In this study, temperature effects are ignored to reduce computational constraint, although significant thermal softening may occur during the initiation of the high explosive event. Material characterisation data for Aluminium 2024-T3 have been investigated and obtained at high strain rates and large strains using the split Hopkinson pressure bar (SHPB) methods[19], as shown in Table 4. The Johnson-Cook parameters have been determined for a strain rate validity range of $\dot{\varepsilon} = 10^{5}$–$10^{-5}\ s^{-1}$.

LS-DYNA has three different constitutive models based on the Johnson-Cook description to describe the bulk material. MAT SIMPLIFIED_JOHNSON_COOK[12] was chosen which excludes the effect of thermal softening and adopts a simple, maximum strain based failure model and is 50% faster than the full Johnson-Cook implementation.

Table 4
Johnson-Cook material model parameters[19]

*MAT_SIMPLIFIED_JOHNSON_COOK MAT_098

Property	Units	Value
ρ	kg/m^3	2,770
υ	–	0·33
E	GPa	73·084
A	MPa	369
B	MPa	684
n	–	0·73
C	–	0·0083
m	–	1·7
T_{room}	K	294
T_{melt}	K	775
C_p	J/kg – K	875

3.3 Modelling the blast load

In this study, a uniformly distributed pressure pulse, similar to that adopted by Karagiozova *et al*[20] given in Equation (2), is analysed which is applied as a pressure pulse on the top surface of the Glare panel.

$$p(t) = p_0 \exp^{-t/t_0} \quad \ldots (2)$$

The pressure decays exponentially with a decay period of t_0 = 0·05 or 0·1ms for the 20 and 40mm charge diameter, respectively. It is assumed that different charge diameters will affect the rate of energy, as defined by the slop of the impulse-time curve, transferred to the target structure which also controls the strain rate experienced by the target material. The effect of changing the exponential decay time constant is shown on a normalised pressure-time curve, given in Fig. 4. The term p_0 is defined as the maximum overpressure of the blast wave which is evaluated based on the momentum conservation equation:

$$I_0 = \mathrm{A}\int_0^{\infty} p(t)\mathrm{d}t \quad \ldots (3)$$

https://doi.org/10.1017/S0001924000007120 Published online by Cambridge University Press

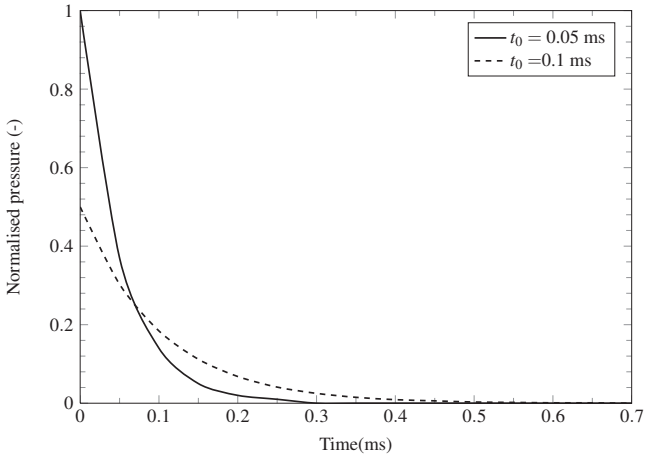


Figure 4. Effect of exponential decay constant on uniformly-distributed pressure profile.

4.0 RESULTS

The predicted and experimental back face mid-point deflections of the clamped Glare 3 panels for the entire tested range of impulses between 11Ns and 31·9Ns is given in Fig. 5. Although the predictive model slightly overestimates the experimental mid-point deflections, reasonable agreement is obtained for all load cases. Considerable inelastic deformation occurred in the panels where yield line formation (the formation of plastic hinges) is clearly seen in Fig. 5, which is typical of the response of a monolithic metal panels subjected to uniformly distributed pressure loading. The overall residual deformation profile obtained from the simulations is shown in Fig. 6.

Experimental observations on the post-damage panels at higher impulses saw an appearance of interfacial debonding and delamination along the boundary edges and significant pulling-in. These observations are related to the presence of clamps and clamp height on impulse transfer to the FML panels, which were ignored in this study. Therefore the results shown in Fig. 6 need to be interpreted in terms of the experimental set-up in which they were obtained, as one might not expect such a steep rise in the deflection profile originating from the clamped boundary edges. Further studies should be performed to incorporate the presence of clamped frames over a range of exposed areas and charge weights/stand-off distances.

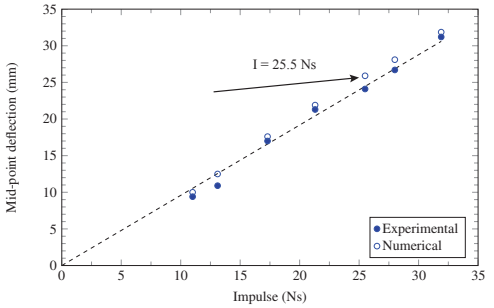


Figure 5. Comparison of experimental and numerical back face mid-point displacements (I = 11Ns – 31·9Ns at 200mm stand-off distance).

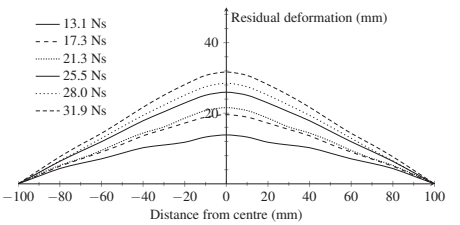


Figure 6. Residual deflection of impulsively loaded Glare 3 panels (I = 11Ns – 31·9Ns at 200mm stand-off distance).

https://doi.org/10.1017/S0001924000007120 Published online by Cambridge University Press

This model also highlights the success in approximating the blast load as a uniformly distributed pressure pulse, expressed as a function of some exponential time decay constant, which corresponds to the mass/diameter of the explosive.

4.1 Comparison with Glare 5 and aluminium 2024-T3

A further objective of this study was to compare the performance of Glare against monolithic aluminium panels of equivalent thickness and Glare 5, a variant of Glare which is used in impact applications, see Table 1 for details on stacking sequence.

The results of this parametric study are given in Fig. 7, which shows mid-point displacement against applied impulse. For a given impulse, it appears that Glare exhibits smaller mid-point displacements than monolithic aluminium panels.

However, direct comparison between all three materials is not possible, due to the inherent differences in density, material properties and configuration. An approach commonly adopted in the literature is to use non-dimensional parameters which allows for comparison of blast-loaded panels of different materials (densities and characteristic stresses), geometries (lengths, widths and thickness's) and loading conditions to be treated similarly. An expression adopted by Langdon *et al*[9] is based on a parameter derived by Nurick and Martin[21] and subsequently modified by Nurick *et al*[22], for localised blast loading and stand-off distance:

$$\alpha_q = \frac{I\left(1+\ln\frac{BL}{\pi R_0^2}\right)}{2t^2\left(1+\ln\frac{S}{R_0}\right)\left(BL\rho\sigma\right)^{1/2}} \qquad \ldots (1)$$

The characteristic stress used in Equation (4) is defined as the static yield stress for monolithic metal plates. However in the case of FML panels, a metal volume fraction (MVF) approach[2] was used to estimate average material properties, such as stress and density. The properties of the component materials are given in Table 5.

Table 5
Glare and Aluminium Material Properties, estimated using the MVF method[2]

	Units	Glare 3-3/2-0·3	Glare 5-3/2-0·3	Al 2024-T3
ρ	(kg/m^3)	2,495	2,360	2,780
σ	(MPa)	305·8	276	369
E	(GPa)	57·3	48·6	72·4

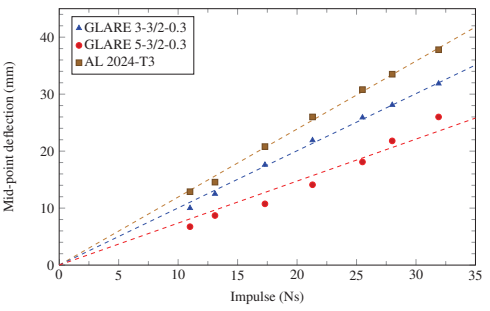


Figure 7. Predicted back face mid-point displacement of Glare 3 and 5 panels and monolithic aluminium plates.

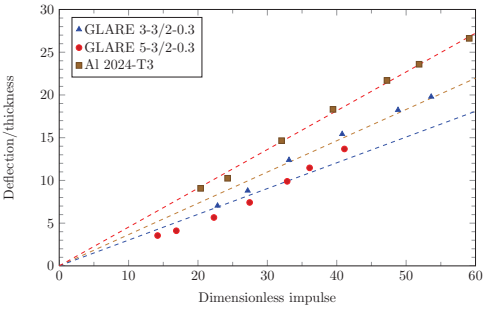


Figure 8. Graph of normalised deflection versus dimensionless impulse.

https://doi.org/10.1017/S0001924000007120 Published online by Cambridge University Press

The results from the parametric blast study were converted to dimensionless form and displayed graphically of displacement-thickness ratio versus dimensionless impulse, as shown in Fig. 8. It is evident that the Glare 5 panels exhibit a smaller normalised displacements (approximately 11% lower) than the monolithic aluminium plates for a given dimensionless impulse.

5.0 CONCLUSION AND FUTURE WORK

A robust and efficient computational model has been developed which is capable of modelling the dynamic non-linear behaviour of Glare panels subjected to blast loadings. Numerical model validation have been performed considering case studies of Glare panels subjected to a blast-type pressure pulse for which experimental data on the back face-displacement and post-damage observations were available.

The aforementioned tests performed by Langdon *et al*[9] highlight the role of well-controlled and well-defined parameters which provide accurate boundary and loading conditions for the complete setup of the simulations with minimal unknown parameters. For example, a simplified approach was used where the experimentally measured transferred impulse was related to a uniformly distributed pressure pulse. Assuming the time duration of the blast wave, this impulsive load could thus be applied directly on the affected area of the structure in the simulations without the need to consider complex empirical blast functions. Quantitative measurements of back face mid-point displacements were provided by the small-scale best tests and compared a posterior with the results of the experiments, showing excellent agreement in terms of dynamic deflection and residual deformation. Evidence of severe yield line deformation was also identified and discussed against the performed blast tests. A parametric study identified Glare as a potential blast attenuating structure, exhibiting superior blast potential against monolithic aluminium plates. The results were normalised and showed that for a given impulse, Glare 3 and 5 exhibited a smaller normalised displacement, outperforming monolithic Aluminium 2024-T3 plates.

However, such well-defined loading conditions are not expected to occur in real-life blast events and may require empirical load functions or a Multi-Material Arbitrary Lagrangian Eulerian (MMALE) approach. Consideration should also be given to the effects of curvature, kinematic boundary and pre-stressed loading conditions which may influence the structural response to blast-type loading. Additionally, interfacial debonding between the metallic/composite interfaces should be taken into consideration to quantify the various energy absorbing mechanisms of these hybrid systems. All of these issues are work that the authors are currently engaged with.

ACKNOWLEDGMENTS

The financial support of the EU-FP6 VULCAN Project (AST5-CT-2006-031011) is gratefully acknowledged.

REFERENCES

1. SOUTIS, C. Recent advances in building with composites, *Plastics, Rubber and Composites*, 2009, **38**, (9-10), pp 59-366.
2. VLOT, A. and GUNNINK, J.W. *Fibre Metal Laminates: An Introduction*, Springer, 2001.

https://doi.org/10.1017/S0001924000007120 Published online by Cambridge University Press

3. VLOT, A. Impact loading on fibre metal laminates, *Int J Impact Engineering*, 1996, **18**, (3), pp 291-307.
4. HOO, F., MICHELLE, S., LIN, CHUNFU., REVILOCK, D.M. and HOPKINS, D.A. Ballistic impact of Glare fiber-metal laminates, *Composite Structures*, 2003, **61**, (1-2), pp 73-88.
5. MCCARTHY, M.A., XIAO, J.R., PETRINIC, N., KAMOULAKOS, A. and MELITO, V. Modelling of bird strike on an aircraft wing leading edge made from fibre metal laminates-part 1: material modeling, Applied composite materials, *Springer*, **11**, (5), pp 295-315.
6. MCMULLIN, D. Lockerbie Insurance, *Scientific American Magazine*, January 2002.
7. FLEISHER, H.J. Design and explosive testing of a blast resistant luggage container, Proc structures under shock and impact conference IV, 1996.
8. NDAMBI, J.M. and DEWOLF, K. and VANTOMME, J. VULCAN Deliverable 2.4: Experimental results for blast behaviour of flat panels, Belgian Royal Military Academy, 2008.
9. LANGDON, G.S., CHI, Y., NURICK, G.N. and HAUPT, P. Response of Glare panels to blast loading, *Engineering Structures*, 2009.
10. KARAGIOZOVA, D., LANGDON, G.S., NURICK, G.N. and CHUNG KIM YUEN, S. Simulation of the response of fibre-metal laminates to localised blast loading, *Int J Impact Engineering*, 2010, **37**, pp 766-782.
11. LANGDON, G.S., LEMANSKI, S.L., NURICK, G.N., SIMMONS, M.C., CANTWELL, W.J and SCHLEYER, G.K. Behaviour of fibre-metal laminates subjVol.cted to localised blast loading: Part I-Experimental observations, *Int J impact Eng*, 2007, **34**, pp 1202-1222.
12. LS-DYNA Keyword Users Manual-Version 971, 2007.
13. HAGENBEEK, M. Characterisation of fibre metal laminates under thermo-mechanical loadings, Delft University of Technology, Delft, The Netherlands, 2005.
14. LINDE, P. and DE BOER, H. Modelling of inter – rivet buckling of hybrid composites, *Composite Structure*, 2006, **73**, pp 221-228.
15. CHANG, F.K. and CHANG, K.Y. Post-failure analysis of bolted composite joints in tension or shear-out mode failure, *J Composite Materials*, 1987, **21**, (809).
16. TSAI, S.W. and WU, E.M. A general theory of strength for anisotropic materials, *J Composite Materials*, 1971, **5**, p 58.
17. JOHNSON, G.R. and COOK, W.H. A constitutive model and data for metals subjected to large strains, high strain rates and high temperatures, Proceedings of the 7th International Symposium on Ballistics, 1983.
18. RAVICHANDRAN, G., ROSAKIS, A.J., HODOWANY, J. and ROSAKIS, P. On the conversion of plastic work into heat during high-strain-rate deformation, American Institute of Physics, 2002.
19. BUYUK, M., KAN, S. and LOIKKANEN, M.J. Explicit finite-element analysis of 2024-T3/T351 aluminum material under Impact loading for airplane engine containment and fragment shielding, *J Aerospace Eng*, 2009, **22**, pp 287-295.
20. KARAGIOZOVA, D., NURICK, G.N. and LANGDON, G.S. Behaviour of sandwich panels subject to intense air blasts-Part 2: Numerical simulation, *Composite Structures*, 2009, **91**, pp 442-450.
21. NURICK, G.N. and MARTIN, J.B. Deformation of thin plates subjected to impulsive loading – a review Part II: Experimental studies, *Int J Impact Eng*, 1989, **8**, pp 171-186.
22. JACOB, N., NURICK, G.N and LANGDON, G.S. The effect of stand-off distance on the failure of fully clamped circular mild steel plates subjected to blast loads, *Engineering Structures*, 2007, **29**, pp 2723-2736.

https://doi.org/10.1017/S0001924000007120 Published online by Cambridge University Press